

# Implicit Solvent Simulations of Peptide Interactions With Anionic Lipid Membranes

Themis Lazaridis

Department of Chemistry, City College of New York/CUNY, New York, New York

**ABSTRACT** A recently developed implicit membrane model (IMM1) is supplemented with a Gouy–Chapman term describing counterion-screened electrostatic interactions of a solute with negatively charged membrane lipids. The new model is tested on peptides that bind to anionic membranes. Pentyllysine binds just outside the plane of negative charge, whereas Lys-Phe peptides insert their aromatic rings into the hydrophobic core. Melittin and magainin 2 bind more strongly to anionic than to neutral membranes and in both cases insert their hydrophobic residues into the hydrocarbon core. The third domain of *Antennapedia* homeodomain (penetratin) binds as an  $\alpha$ -helix in the head-group region. Cardiotoxin II binds strongly to anionic membranes but marginally to neutral ones. In all cases, the location and configuration of the peptides are consistent with experimental data, and the effective energy changes upon binding compare favorably with experimental binding free energies. The model opens the way to exploring the effect of membrane charge on the location, conformation, and dynamics of a large variety of biologically active peptides on membranes. *Proteins* 2005;58:518–527. © 2004 Wiley-Liss, Inc.

**Key words:** implicit solvation; molecular dynamics simulations; pentyllysine; melittin; magainin 2; pAntp (penetratin); cardiotoxin

## INTRODUCTION

Interactions of peptides with lipid membranes are featured in numerous biological processes. For example, antimicrobial peptides bind and permeabilize membranes causing bacterial death.<sup>1</sup> Fusion peptides are thought to insert at an oblique angle and destabilize membranes leading to membrane fusion.<sup>2</sup> Cell penetrating peptides are highly charged basic peptides with a mysterious way of translocating across the cell membrane without the involvement of a receptor.<sup>3</sup> The interaction of signal sequences with lipid membranes may play a role in protein localization and export.<sup>4</sup> Amyloid formation has been found to be accelerated by lipid membranes<sup>5</sup> and amyloid toxicity in neurological diseases may be caused by membrane permeabilization.<sup>6</sup>

Many experimental techniques, including neutron and X-ray diffraction, fluorescence spectroscopy, CD, oriented CD, calorimetry, spin-labeling EPR, solid-state NMR, or

solution NMR in micelles, have been employed to characterize the interaction of peptides with membranes. Because most of these techniques give only low-resolution structural information, modeling can be a useful complement of experimental studies. MD simulations using an explicit representation of the lipids and water provide the most detailed information.<sup>7,8</sup> However, even very long (by current standards, 20–30 ns) simulations of peptide–bilayer systems give results dependent on the initial conditions and are thus unable to predict the optimal location and conformation of a peptide with respect to a membrane.<sup>9,10</sup> That would be possible with a method that provides the free energy of alternative configurations. Numerical solutions of the PB equation are one way to do this, since they provide the electrostatic free energy for a given peptide conformation in water or a low-dielectric slab in water. Complemented with a model for the hydrophobic interaction, these calculations provide the effective energy as a function of position and orientation.<sup>7,11–15</sup> The main limitation of PB is that it does not easily allow for peptide flexibility; that is, it is almost always carried out using a fixed peptide conformation (it is quite expensive to perform MD simulations with a PB energy). In principle, it is possible to perform PB calculations on a large number of conformations generated by Monte Carlo or MD in vacuum, but such a procedure will bias the sampling toward conformations that are favorable in vacuum and may omit conformations that are stabilized by the interface.

These difficulties led to the proposition of simpler, semiempirical models for the membrane.<sup>16–24</sup> Most of these models give the energy as a function of position and orientation with respect to a bilayer for a given peptide or protein conformation, but not the effective energy of

**Abbreviations:** 1D, one-dimensional; CD, circular dichroism; DOPC, dioleoylphosphatidylcholine; DPC, dodecylphosphocholine; EPR, electron paramagnetic resonance spectroscopy; GB, Generalized Born; GC, Gouy–Chapman; MD, molecular dynamics; NOE, nuclear Overhauser effect; pAntp, *Antennapedia* homeodomain third helix; PB, Poisson–Boltzmann; PC, phosphatidylcholine; RMSD, root-mean-square deviation.

Grant sponsor: National Science Foundation; Grant number: MCB-0316667. Grant sponsor: NIH (RCMI grant); Grant number: 5G12RR003060 (for computational resources).

Correspondence to: Themis Lazaridis, Department of Chemistry, City College of New York/CUNY, 138th Street and Convent Avenue, New York, NY 10031. E-mail: tlazaridis@ccny.cuny.edu

Received 22 July 2004; Accepted 13 September 2004

Published online 17 December 2004 in Wiley InterScience (www.interscience.wiley.com). DOI: 10.1002/prot.20358

different conformations. We recently proposed an energy function (IMM1) that is designed to do both.<sup>25</sup> Far from the membrane, the function is equivalent to EEF1,<sup>26</sup> a well-tested model for aqueous solution. It can therefore be used to study the folding process of membrane proteins.

A rival approach, similar in spirit, involves the extension of the GB solvation model to membranes.<sup>27,28</sup> The key difference between the two methods is in the treatment of electrostatic interactions: IMM1 employs the less rigorous, linear, distance-dependent dielectric constant in water, with an empirical adjustment inside the membrane, while the GB method uses the GB approximation. The self-energy is also treated differently by the two methods. GB calculates separately the electrostatic and nonpolar contributions, and assumes that the latter is proportional to the solvent-exposed surface area, while IMM1 does not separate the two and uses experimental transfer free energies for the self-energies. In its present form, the GB method neglects the favorable protein–lipid interactions, but this can be easily fixed. Also, the GB model seems to give energies of binding to membranes that are too large compared to experimental partition coefficients (an energy minimum of 31 kcal/mol is reported for melittin at the membrane interface<sup>28</sup>). While the computational expense of both methods is very low, IMM1 is about twice as fast. The merits and weaknesses of each approach will become clearer as they are applied to different problems.

The implicit membrane models developed so far neglect any electrostatic interactions between the solute and the lipid headgroups. This is probably a good approximation for zwitterionic lipids. However, most biological membranes contain a significant fraction of anionic lipids, such as phosphatidylglycerol, phosphatidylserine, phosphatidic acid, or cardiolipin.<sup>29</sup> A large number of basic peptides and peripheral membrane proteins interact with membranes via electrostatic interactions. Such systems have been studied with the PB equation using an idealized, regular lattice of lipid molecules to model the membrane and rigid conformations for the peptides or protein.<sup>30–32</sup> As mentioned above, this approach is limited by the assumption of a fixed conformation and by some difficulty in studying hydrophobic insertion together with electrostatic interactions.

Here we present an extension of IMM1 to anionic membranes via addition of a term derived from the GC theory of the electrostatic double layer.<sup>33,34</sup> We refer to this model as IMM1-GC. The initial tests reported here show good agreement with available experimental data, both structural and thermodynamic. Pentyllysine binds outside the headgroup region whereas K3F2 buries its aromatic groups in the hydrophobic core. Melittin and magainin bind both anionic and zwitterionic membranes but exhibit a higher affinity for anionic membranes. The difference in binding free energy is consistent with experimental binding constants. Penetratin binds anionic but not zwitterionic membranes. Cardiotoxin II binds strongly to anionic but marginally to neutral membranes, and its configuration on the membrane is consistent with experimental data.

## METHODS

### IMM1

IMM1 is an extension of EEF1, an effective energy function for soluble proteins,<sup>26,35</sup> describing the effective energy of a protein solute in a lipid membrane:

$$W_{\text{IMM1}} = E + \Delta G^{\text{solv}} \quad (1)$$

where  $E$  is the intramolecular energy of the solute, given by a modified form of the CHARMM polar hydrogen force field,<sup>36</sup> and  $\Delta G^{\text{solv}}$  is the solvation free energy, given by

$$\Delta G^{\text{solv}} = \sum_i \Delta G_i^{\text{solv}} = \sum_i \Delta G_i^{\text{ref}} - \sum_i \sum_{j \neq i} g_i(r_{ij}) V_j, \quad (2)$$

where  $\Delta G_i^{\text{solv}}$  is the solvation free energy of atom  $i$ ,  $r_{ij}$  is the distance between  $i$  and  $j$ ,  $g_i$  is the solvation free energy density of  $i$  (a Gaussian function of  $r_{ij}$ ),  $V_j$  is the volume of atom  $j$ , and  $\Delta G_i^{\text{ref}}$  is the solvation free energy of an isolated atom. In addition, EEF1 employs a distance-dependent dielectric constant ( $\epsilon = r$ ) and a neutralized form of the ionic side-chains.

In IMM1,  $\Delta G_i^{\text{ref}}$  is a linear combination of values for water and for cyclohexane (which models the nonpolar core of the membrane)<sup>25</sup>:

$$\Delta G_i^{\text{ref}}(z') = f(z') \Delta G_i^{\text{ref, wat}} + [1 - f(z')] \Delta G_i^{\text{ref, chex}}, \quad (3)$$

where  $z' = |z|/(T/2)$ , and  $T$  is the thickness of the nonpolar core of the membrane. The function  $f(z')$  describes the transition from one phase to the other:

$$f(z') = \frac{z'^n}{1 + z'^n} \quad (4)$$

The exponent  $n$  controls the steepness of the transition. A value of 10 gives a region of 6 Å, over which the environment goes from 90% nonpolar to 90% polar (the “interface”). The midpoint of the transition ( $f = 0.5$ ) corresponds to the hydrocarbon–polar headgroup interface (roughly the level of the ester carbonyls in phospholipids). The strengthening of electrostatic interactions in the membrane is effected by a modified dielectric screening function

$$\epsilon = r^{f_{ij}} \quad (5)$$

where  $r$  is the distance in angstrom units (but  $\epsilon$  is dimensionless), and  $f_{ij}$  depends on the position of the interacting atoms with respect to the membrane. Far from the membrane,  $f_{ij}$  is equal to 1, and we recover the linear distance-dependent dielectric model. For  $f_{ij}$ , we employed the empirical model

$$f_{ij} = a + (1 - a) \sqrt{f(z_i) f(z_j)}, \quad (6)$$

with  $a$  being an adjustable parameter. The value  $a = 0.85$  was found to give membrane insertion or adsorption energies of the expected order of magnitude.<sup>25</sup>

### Gouy–Chapman Theory

The published form of IMM1 does not account for any electrostatic interactions between the lipid headgroups

and the solute. To incorporate this effect, we resort to the venerable GC theory for the electrical double layer.<sup>33</sup> The GC theory results from the solution of the (nonlinear) PB equation for the 1D system of a planar surface with a uniform (“smeared”) charge next to an electrolyte solution. The equations are simplest for a symmetric electrolyte, for which the surface potential,  $\psi(0)$ , is given by

$$\sinh \left[ \frac{ze\psi(0)}{2kT} \right] = \frac{\sigma}{\sqrt{8\epsilon_a\epsilon_o kT\rho}}, \quad (7)$$

where  $z$  is the valence of the electrolyte,  $e$  is the charge of a proton,  $\sigma$  is the surface charge density,  $\epsilon_a$  is the relative permmissivity (80 for water),  $\epsilon_o$  is the permmissivity of vacuum,  $k$  is Boltzmann’s constant,  $T$  is the absolute temperature, and  $\rho$  is the number of ions per volume ( $\rho = 1000 N_{av} c$ , where  $c$  is the molarity). The potential as a function of distance  $r$  outward from the charge surface is

$$\frac{ze\psi(r)}{2kT} = \ln \frac{[1 + \alpha \exp(-\kappa r)]}{[1 - \alpha \exp(-\kappa r)]},$$

$$\text{where } \alpha = \frac{\exp(e\psi(0)/2kT) - 1}{\exp(e\psi(0)/2kT) + 1}, \quad (8)$$

and  $\kappa$  is the inverse Debye length, which for a symmetric electrolyte is

$$\kappa = \sqrt{\frac{2\rho o z^2 e^2}{\epsilon_a \epsilon_o kT}}, \quad (9)$$

where  $\rho$  is the number of ions per volume ( $\rho = 1000 N_{av} c$ ). The charge plane is assumed to be  $O$  Å outward from the nonpolar–polar interface ( $O$  is referred to as “offset”). If  $z = 0$  is the midplane of the membrane,  $T$  is the thickness of the hydrocarbon region, and  $O$  is the offset, then  $r = |z| - T/2 - O$ . The potential inward from the charge plane (inside the membrane) is constant and equal to the surface potential, that is,  $\psi(z) = \psi(0)$  for  $|z| < T/2 + O$ . No smoothing is done at the boundary.

The electrostatic interaction energy of a peptide in this electrostatic field is given by the sum over all atoms of the product of the electrostatic potential at that point, with the partial charge of the atom,  $q_i$ :

$$E_{GC} = \sum_i \psi(z_i) q_i. \quad (10)$$

Analytical derivatives of the above term with respect to the  $z$  coordinate are readily obtained and MD simulations are thus straightforward.

These equations are implemented into the CHARMM program, versions c32a1 and c31b1. The user specifies the mol fraction of anionic lipids ( $f_a$ ), the area per lipid ( $A$ ), the salt concentration, the valence of the electrolyte (only symmetric ions are considered for now), and the position of the plane of smeared charge relative to the nonpolar–polar interface (offset). The surface charge density is calculated from the mol fraction of anionic lipids:  $\sigma = f_a * e * z/A$ . Note that the ionic side-chains carry a full charge in the calculation of the GC term but are net neutral in the calculation of intra- and interpeptide interactions, as

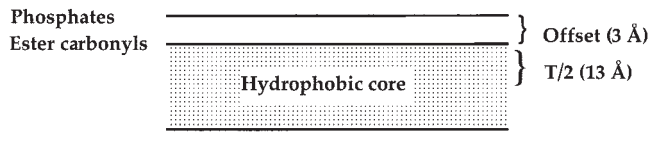


Fig. 1. Schematic of the implicit membrane model. The inner lines denote the hydrocarbon–polar interface and the outer lines the plane of negative charge.

required by the EEF1 model. This is accomplished by adding a full charge to the NZ atom of Lys or the 2 NC2 atoms of Arg, or the N atom of the N-terminus and subtracting a full charge from the CG of Asp or CD of Glu, or C of the C-terminus when the GC term is calculated. The calculations reported here were performed with an offset of 3 Å (i.e., if  $T = 26$  Å, then the hydrophobic–hydrophilic interface is at  $z = \pm 13$  and the smeared charge at  $z = \pm 16$  Å). Unless otherwise noted, a 0.1 M salt concentration was used.  $A$  was set to 70 Å<sup>2</sup>,<sup>31</sup> which is close to the best experimental values for DOPC and Egg PC.<sup>37</sup> Small variations in  $A$  are equivalent to small variations in the anionic fraction and do not affect the results significantly. For best accuracy,  $A$  should be adjusted to reflect experimental or simulation data for the membrane of interest.

Figure 1 shows a schematic of the present membrane model. The hydrophobic core is delimited by the plane of average location of the lipid ester carbonyls (inner lines). This is the midpoint ( $f = 0.5$ ) of transition from the nonpolar to the polar solvent region. The outer lines denote the plane of the phosphates (the plane of smeared charge for the GC model). In this work, we only consider interfacial peptide binding; thus, the thickness of the hydrophobic core plays no role. In the remaining figures, only the upper leaflet of the membrane will be shown.

## Results on Test Systems

All simulations were done at 300 K using the CHARMM program, SHAKE for the bonds involving H, and a 2-fs timestep. The reported average effective energy differences between membrane-bound and aqueous states are not directly comparable to experimental binding free energies, because they do not include the translational and rotational entropy cost of binding. However, these terms have been estimated to be about +1.3 kcal/mol for interfacial binding.<sup>38</sup> Therefore, the effective energy difference should be about 1.3 kcal/mol more negative than experimental binding free energies if no conformational changes are involved (note that small standard-state corrections may also be needed<sup>39</sup>). The common standard states for membrane binding free energies are summarized in the Appendix. Complete calculations of the free energy with more precise estimates of the entropic contributions are currently in progress.

## Lys and Lys-Phe pentapeptides

The interaction of Lys oligopeptides with anionic membranes has been studied both experimentally and theoret-

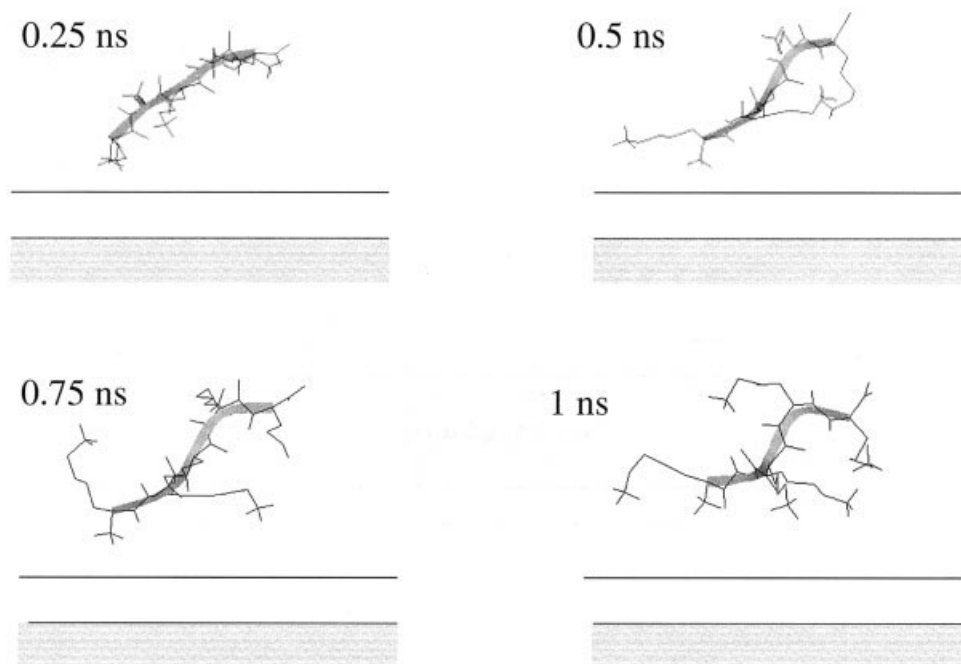


Fig. 2. Snapshots from a 1-ns simulation of pentalysine on an anionic membrane. The shaded region denotes the hydrocarbon core and the outer line, the plane of smeared negative charge.

cally using numerical solutions of the PB equation.<sup>40</sup> It was found that they interact with 33% acidic lipids but do not penetrate the polar headgroup region of the membrane. Here, pentalysine was built in an extended conformation and placed at the hydrocarbon boundary, with the side-chains parallel to the membrane (30% anionic). A 20-ps MD simulation with harmonic constraints on the backbone atoms was followed by a 1-ns unconstrained simulation. A 1-ns simulation was also performed for the same peptide in water. The center of mass of the peptide stabilizes to  $z = 22\text{--}23$  Å after about 20 ps (the phosphate plane is at 16 Å). Four snapshots from the trajectory are shown in Figure 2. While the peptide does not maintain a well-defined conformation, it remains just outside the headgroup region, with several Lys side-chains a few angstrom units from the phosphate plane. Figure 3 plots the effective energy (averaged over 2-ps intervals) as a function of time and the cumulative average effective energy. The average effective energy of the membrane-bound state over the last 900 ps is 3.3 kcal/mol lower than in water (see Table I). The favorable energy change upon membrane binding is entirely due to the GC term, whose average value is  $-4.6$  kcal/mol. Similar results are obtained by the PB method.<sup>38</sup> The experimental binding free energy of pentalysine to 33% anionic membrane was reported to be  $-5$  kcal/mol in one experiment.<sup>40</sup> Other experiments using blocked pentalysine (Ac-K5-NH<sub>2</sub>) gave  $-3.4$  kcal/mol.<sup>41</sup> For blocked pentalysine, we obtain  $\Delta\langle W \rangle = -2.7$  kcal/mol. This underestimation of binding affinity may be due to the neglect of lipid demixing (i.e., the ability of the peptide to concentrate acidic lipids around it).<sup>42</sup> Simulations at 0% acidic lipids show that pentalysine does not bind to neutral membranes

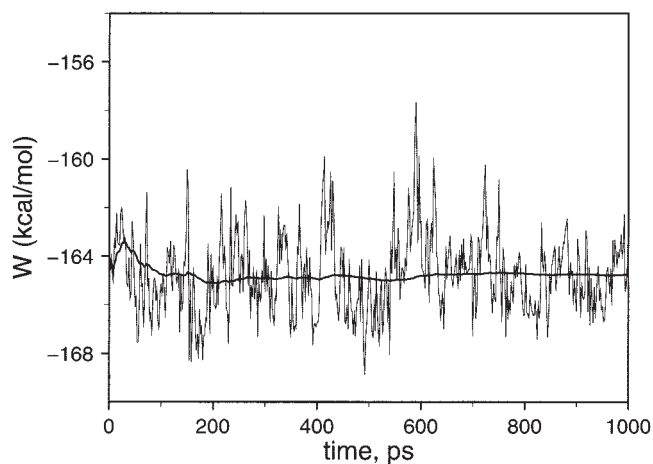


Fig. 3. Effective energy (averaged over 2-ps intervals) as a function of simulation time (thin line) and cumulative average effective energy (thick line) for pentalysine on an anionic membrane.

(its center of mass goes to  $z = 32$  Å after 200 ps of MD simulation), in agreement with experiment.

Victor and Cafiso<sup>41</sup> studied similar pentapeptides with one or more of the Lys replaced by Phe. The peptides also incorporated into the backbone a rigid nitroxide label as an EPR reporting group. This work confirmed that pentalysine binds outside the membrane, but the Phe-containing peptides were found to insert into the membrane (the label was placed 8–9 Å below the phosphate level). Figure 4(A and B) shows two snapshots of the Ac-KFKFK-NH<sub>2</sub> peptide (modeled without the spin label) from a 1-ns MD simulation on a 30% anionic membrane. The 2 phenylalanines are indeed inserted into the nonpolar membrane core, although not as



TABLE I. Average Effective Energies (kcal/mol)<sup>a,b,c</sup>

	K5	K3F2	Melittin	Magainin	pAntp <sup>d</sup>	Cardiotoxin <sup>d</sup>
$\langle W \rangle$ on mem	$-164.8 \pm 0.2$	$-124.6 \pm 0.2$	$-508.4 \pm 0.5$	$-495.6 \pm 0.3$	$-400.5 \pm 0.5$ $-398.2 \pm 0.4$ $-403.0 \pm 0.5$ $-399.2 \pm 0.4$	$-1154.8 \pm 0.6$ $-1157.5 \pm 0.8$ $-1158.3 \pm 0.4$ $-1159.9 \pm 0.4$
$\langle E_{gc} \rangle$	$-4.6 \pm 0.03$	$-2.6 \pm 0.03$	$-2.1 \pm 0.02$	$-3.05 \pm 0.03$	$-8.2 \pm 0.12$ $-8.0 \pm 0.05$ $-8.9 \pm 0.11$ $-8.0 \pm 0.08$	$-16.6 \pm 0.11$ $-16.0 \pm 0.35$ $-17.2 \pm 0.12$ $-17.1 \pm 0.10$
$\langle W \rangle$ in water	$-161.5 \pm 0.2$	$-120.6 \pm 0.2$	$-495.6 \pm 0.5$	$-487.3 \pm 0.3$	$-394.5 \pm 0.3$	$-1132.7 \pm 0.4$
$\Delta \langle W \rangle$	$-3.3 \pm 0.3$	$-4.0 \pm 0.3$	$-12.8 \pm 0.7$	$-8.3 \pm 0.4$	$-5.7 \pm 1.8^e$	$-24.9 \pm 1.8^e$
$\langle W \rangle$ neu mem		$-121.7 \pm 0.2$	$-503.6 \pm 0.6$	$-492.8 \pm 0.3$		
$\Delta \langle W \rangle$ neu mem		$-1.1 \pm 0.3$	$-8 \pm 0.8$	$-5.5 \pm 0.4$		

<sup>a</sup>Absolute energies are meaningless but are given for concreteness.

<sup>b</sup>Averages were calculated over the last 900 ps of a 1-ns simulation.

<sup>c</sup>Error bars are  $2 \times$  standard deviation of the mean.

<sup>d</sup>The 4 values are results of simulations starting from 4 different orientations.

<sup>e</sup>Calculated using the average over the 4 orientations.

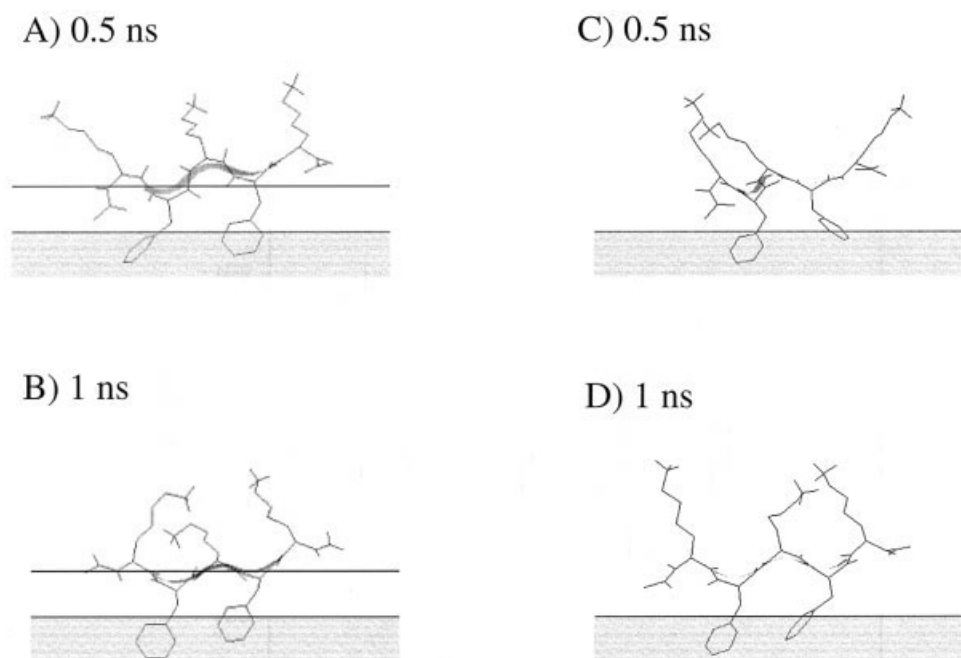


Fig. 4. The structure of KFKF-NH<sub>2</sub> on an anionic membrane (A and B) and a neutral membrane (C and D).

deeply as estimated by EPR (the CZ atoms of the Phe are 3–4 Å below the charge plane). The center of mass of the peptide remains close to  $z = 17$  Å throughout the simulation. The effective energy on the membrane is 4 kcal/mol lower than in water, of which 2.6 kcal/mol is contributed by the GC term (see Table I). The experimental binding free energy is -3.84 kcal/mol.<sup>41</sup> The experimental finding that K3F2 binds slightly more strongly than K5 is reproduced by the calculations. The peptide also binds to neutral membranes [Fig. 4(C and D)], but the binding energy is much lower ( $\Delta \langle W \rangle = -1.1$  kcal/mol). This is also in agreement with experiment, which finds that K3F2 binds to neutral membranes, with a binding free energy of -1.4 kcal/mol at the most (partition coefficient < 10).<sup>41</sup>

The above results were obtained using a starting configuration with all side-chains flat on the membrane interface. Surprisingly, a simulation starting with the Lys side-chains pointing toward and the Phe side-chains pointing away from the membrane, fails to lead to Phe insertion in 1 ns. Apparently, there is a significant barrier for flipping. The average effective energy in this case is 1.5 kcal/mol higher than that of the original simulation. Thus, one can select the optimal configuration based on energetics.

#### Melittin and magainin

Simulations of melittin on neutral membranes have been reported in the original IMM1 publication.<sup>25</sup> Melittin contains 3 Lys and 2 Arg; consequently, its affinity for

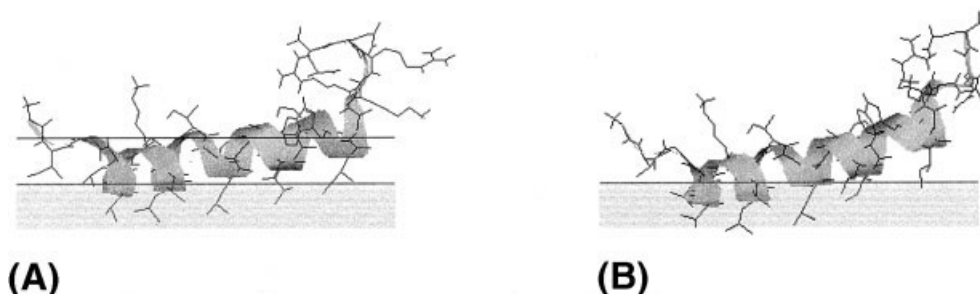


Fig. 5. Melittin on an anionic membrane (A) and a neutral membrane (B). Minimized average structures.

anionic membranes is 1 to 2 orders of magnitude larger than that for neutral membranes,<sup>43–45</sup> which corresponds to a 1.4–2.8 kcal/mol larger binding free energy. Specifically, the binding free energy of melittin is  $-5.1$  kcal/mol for neutral membranes<sup>44</sup> and  $-6.6$  kcal/mol for 10% anionic membranes.<sup>45</sup>

Starting from the initial configuration of Bernéche et al.,<sup>7</sup> melittin was subjected to a 1-ns MD simulation on a 10% anionic membrane at 0.1 *M* salt. The molecule attained a conformation similar to that previously reported on a neutral membrane, that is, an interfacial helix with a disruption at the C-terminus [Fig. 5(A)]. The disruption is caused by the presence of 4 consecutive charged residues that cannot fit into an amphipathic pattern. The corresponding neutral membrane simulation gave a similar conformation [Fig. 5(B)]. The average effective energies are reported in Table I. The energy is 4.8 kcal/mol lower in the anionic membrane, while the average GC energy on the anionic membrane was  $-2.1$  kcal/mol. The remainder is due to small differences in the conformational ensembles sampled.

Comparison with the experimental binding free energies is complicated by the fact that the experiment measures the free energy of the transition “random coil in water”  $\rightarrow$  “helix in the membrane,” and the free energy difference between coil and helix is difficult to compute. Instead we focus on the transition “helix in water”  $\rightarrow$  “helix on the membrane.” The free energy of helix formation in water should be small and positive for melittin, not more than 2–3 kcal/mol. The average effective energy of melittin as a helix in water was computed from a 1-ns simulation with soft harmonic constraints (to preserve helicity) starting from the crystal structure. The value reported in Table I is 8 kcal/mol lower than the value in the neutral membrane. This difference is of the expected order of magnitude given the above considerations.

Magainin 2 is an antimicrobial peptide that permeabilizes bacterial membranes but, unlike melittin, is not hemolytic. It also has several basic residues and thus binds preferentially to anionic membranes ( $\Delta G^\circ = -5.6$  kcal/mol for 75:25 POPC:POPG, calculated as  $-RT\ln K_{app}$ <sup>46</sup>). However, contrary to a widespread impression, it also binds to neutral membranes with a  $\Delta G^\circ$  of  $-4.6$  kcal/mol.<sup>47</sup> Magainin 2 amide (GIGKFLHSKKF-GKAFVGEIMNS-NH<sub>2</sub>) was built as an ideal  $\alpha$ -helix and placed at the membrane interface with the hydrophobic

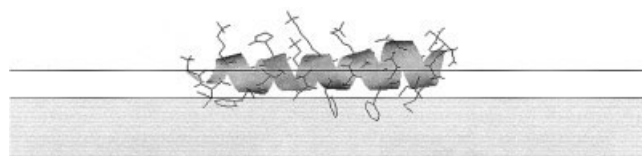


Fig. 6. Magainin 2 on an anionic membrane. Minimized average structure.

face inwards. A 20-ps MD simulation with harmonic constraints on the backbone was followed by unconstrained 1-ns simulations. For both neutral and 30% anionic membranes, the peptide remained bound as a helix with the 3 Phe residues and the Met inserted into the nonpolar core (Fig. 6). In both cases, some  $\pi$  helical character is observed near the C-terminal end of the molecule. For the neutral membrane, the average effective energy was 5.5 kcal/mol lower than that in water (Table I). For the charged membrane, it was 8.3 kcal/mol lower, and the average GC energy was about  $-3.05$  kcal/mol. Again, these values are consistent with the experimental affinities. The difference in binding free energy is expected to be smaller than the difference in effective energy, because stronger interactions may lead to lower conformational entropy.

### pAntp

The third helix of the *Antennapedia* homeodomain (pAntp or “penetratin”) belongs to an intriguing class of basic peptides (“cell-penetrating peptides”) that seem to have the ability not only to traverse lipid membranes but also carry along molecules of varying size attached to them.<sup>3</sup> pAntp binds to negatively charged phospholipid vesicles and adopts an  $\alpha$ -helical conformation<sup>48,49</sup> parallel to the membrane surface.<sup>50</sup> The binding free energy (calculated as  $-RT\ln K_{app}$ ) was measured as  $-9.6$  kcal/mol for 40% anionic membranes and  $-5.8$  kcal/mol for 10% anionic membranes.<sup>49</sup> The peptide does not bind effectively to membranes with less than 10% anionic lipids.<sup>48</sup>

As a helix, pAntp (RQIKIWFQNRRMKWKK) is imperfectly amphipathic. A cluster of hydrophobic residues is formed on one face (I3, W6, F7, and W14), but R10 falls right in the middle of this face. For this reason, it does not bind to our neutral membrane (placed at the interface as a helix and simulated for 100 ps, it moves rapidly away from

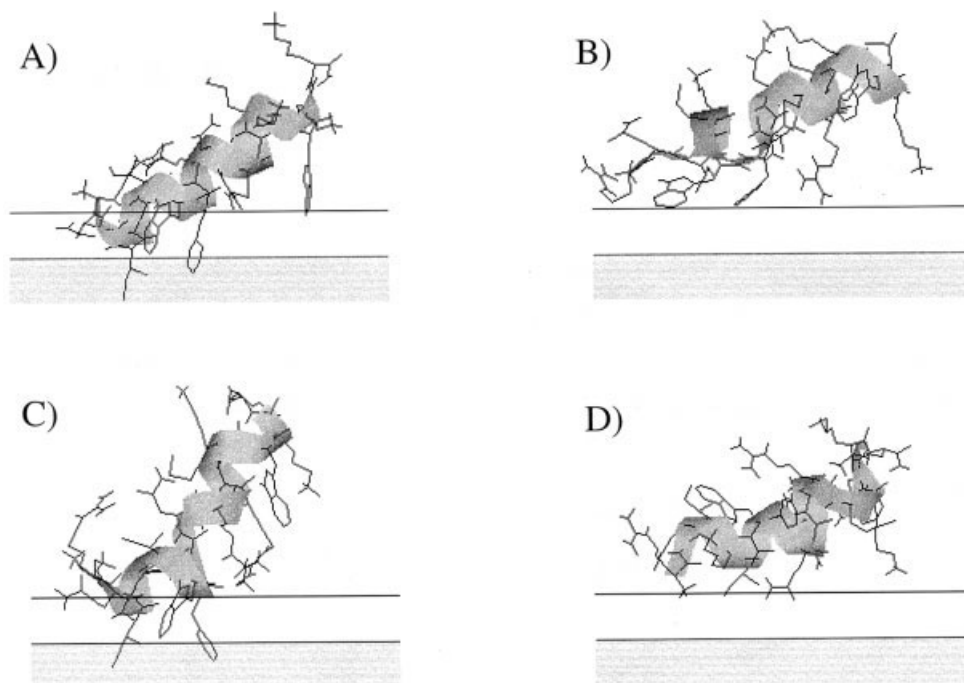


Fig. 7. The pAntp peptide on an anionic membrane; final structures are from simulations starting from 4 different orientations.

the membrane). In contrast, simulations on a 40% anionic membrane led to binding in the headgroup region. Because of the low amphipathicity, 4 different orientations with respect to the membrane were each subjected to a 1-ns MD simulation. The final structures are shown in Figure 7. Three of the 4 runs give very similar structures, showing an oblique orientation, with the N-terminal end closer to the hydrophobic core of the membrane. In 2 of the 3, Ile3 and Phe7 partially insert into the hydrophobic core. This orientation is similar to Brattwall et al. (Fig. 2B<sup>50</sup>) except that it is not as deep in the membrane because of interference by Arg 10. The fourth orientation is “flipped over,” with the Ile3 and Phe7 exposed to water, and Ile5 and the N-terminus toward the membrane.

Experiments suggest a less than 100% helical conformation,<sup>49,50</sup> while we observe essentially perfect helices. This may be due to an overstabilization of  $\alpha$ -helices in our force field, although there is some evidence that CD underestimates the helical content in membrane-mimetic media.<sup>51</sup> The average effective energies over the 4 runs are shown in Table I. The “flipped” orientation has similar energy to the other runs. The GC energy ranges from  $-8.0$  to  $-8.9$  kcal/mol, but the membrane-bound state is only, on average,  $-5.7$  kcal/mol lower in energy than the helix in water, because of the cost of partially desolvating the charged groups. This value seems a bit low compared to the binding free energies mentioned above. Thus, for this peptide, the model reproduces the selective binding to anionic membranes but underestimates the binding strength. Again, this may be due to the neglect of anionic lipid clustering.

### Cardiotoxin

Cardiotoxins are components of the cobra venom with 60–62 residues that interact with and depolarize cell membranes. Several structures have been solved by crystallography or NMR. They contain exclusively  $\beta$  structure, stabilized by 4 disulfide bonds. They have an excess of basic residues and, therefore, interact preferentially with anionic membranes. They are divided into 2 classes, S-type and P-type, with the latter exhibiting higher affinity for membranes.<sup>52</sup> The P-type cardiotoxins were found to bind zwitterionic micelles or sonicated vesicles.<sup>52–54</sup> However, the latest experiments suggest a negligible interaction with well-formed, well-hydrated zwitterionic bilayers.<sup>55,56</sup> A previous modeling study<sup>57</sup> based on a different implicit membrane model used a transmembrane potential to mimic the effect of anionic lipids, but this is rather inappropriate. Another study used an electrostatic potential obtained from explicit lipid simulations and performed an energy map as a function of cardiotoxin orientation next to a membrane.<sup>56</sup>

Here we performed simulations of cardiotoxin II from *Naja oxiana*, whose structure has been determined in DPC micelles (PDB code: 1FFJ).<sup>58</sup> The molecule was oriented with its principal axis in the  $x$  direction and then moved 25 Å in the  $z$  direction. One-nanosecond simulations on a 100% anionic membrane started from 4 different orientations, obtained by rotating around the  $x$  axis in 90° increments. The final structures were very similar regardless of the initial orientation (Fig. 8). Hydrophobic residues from the 3 loops partially insert into the membrane, and several basic residues interact with the phosphate charges.

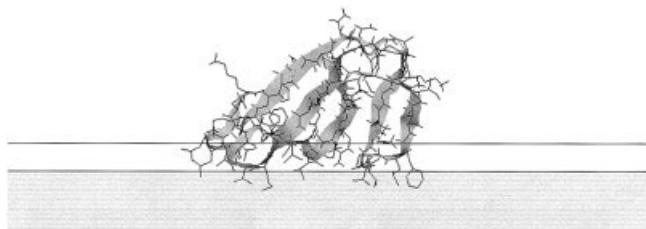


Fig. 8. The structure of cardiotoxin II on an anionic membrane after 1 ns of simulation. The results of the other 3 runs are similar.

The  $\beta$ -sheet adopts an oblique orientation with respect to the membrane. This structure is in agreement with a number of experimental results: (1) Fluorescence and NMR studies in micelles suggest that the tips of the loops interact with the lipids<sup>52,58</sup>; (2) FTIR studies obtained an angle of  $48 \pm 20^\circ$  between the  $\beta$ -sheet plane and the bilayer normal<sup>56</sup>; (3) intermolecular transfer NOEs have been observed between the tyrosines and the membrane headgroups, indicating that the face of the  $\beta$ -sheets that exposes these tyrosines is oriented toward the membrane.<sup>56</sup> This is what we observed here as well.

A 1-ns simulation was also performed in pure water (far from the membrane). The average effective energy in the membrane is about 25 kcal/mol lower than in water (see Table I). Most of this is contributed by the GC term, which is 16–17 kcal/mol. Of course, for physiological membranes, which are not 100% anionic, this contribution will be smaller. The remainder of the binding energy is contributed by hydrophobic side-chain burial into the membrane and some enhancement of the electrostatic interactions. The program DSSP<sup>59</sup> detects 5–9 more hydrogen bonds in the membrane-bound structures than in the aqueous structure after dynamics. Some of the extra hydrogen bonds are located in the loops that insert into the membrane. This seems consistent with the experimental finding that  $\beta$  structure is enhanced upon binding to membranes.<sup>60</sup>

The simulations were repeated for a neutral membrane. For 3 initial orientations, the peptide moved rapidly away from the membrane. In the fourth, it remained close to the membrane and gave a final structure with only the Leu47 side-chain inserted into the membrane. The energy of that configuration was 3.6 kcal/mol lower than the same conformation in water. This marginal interaction with neutral membranes is in agreement with the recent experiments mentioned above.<sup>55,56</sup> The RMSDs of all final structures from the initial NMR structure (model 1 from 1FFJ.pdb) were between 1.2 Å and 1.7 Å for the backbone (except for one neutral membrane run, 2.4 Å) and 1.9–2.6 Å for all atoms (except for that same run, 3.15 Å). Thus, binding to the membrane does not lead to major rearrangements in the structure of the peptide.

## CONCLUSIONS

The GC theory has a long list of applications in colloid science and biophysics.<sup>33,34,61</sup> This is apparently the first time that it has been used as a potential in MD simula-

tions. The theory is based on the nonlinear PB equation and therefore is not limited to low potentials. However, it treats ions as point charges and neglects ion–ion correlations. Furthermore, it assumes a flat surface and a uniform distribution of the charge (“smeared” charge approximation). Experimental tests have shown that the theory works surprisingly well.<sup>33</sup> In using the GC theory, we neglect not only discrete charge effects but also possible effects from lipid demixing (i.e., loss of uniformity in the distribution of charged and uncharged lipids in the membrane).<sup>42</sup> Also, the model applies only to nonspecific electrostatic interactions; no discrimination is made between lipids with the same charge but different structure (except, the position of the charge plane can differ). One possible way to account for specific binding is the Gouy–Chapman–Stern theory, which incorporates an experimentally determined binding constant.<sup>33</sup> Finally, the present implementation of GC theory neglects any perturbation to the electrostatic potential caused by the peptide. This may be important for large proteins that penetrate the membrane and displace phospholipid headgroups. It might be possible to develop corrections for this based on solutions of the PB equation.

IMM1-GC seems to give excellent results, not only on the qualitative behavior of peptides at the membrane–water interface but also on the quantitative aspects of membrane binding. The changes in effective energy upon binding are quite reasonable compared to experimental binding free energies. In several tests, however, they seem to be a bit low. This may be due to the neglect of lipid demixing mentioned above, and could be remedied by incorporating theoretical results on this effect.<sup>42</sup> In addition, we are currently working toward an accurate estimation of the entropic contributions to binding. That will enable a more precise comparison with experimental binding free energies and further fine-tuning of the model.

The ability to model charged membrane–peptide interactions with full conformational flexibility of the peptide opens the way to the study of a large variety of membrane active peptides, such as antimicrobial peptides, fusion peptides, amyloid forming peptides, and so forth. Modeling studies may provide valuable input for interpretation of biophysical experiments and may yield fundamental physical insights. Such insights may be useful in understanding phenomena such as  $\beta$ -sheet formation on membranes.<sup>62</sup>

## ACKNOWLEDGMENTS

I am grateful to Marilyn Gunner and Tom Haines for being great, membrane-loving colleagues.

## REFERENCES

1. Zasloff M. Antimicrobial peptides of multicellular organisms. *Nature* 2002;415:389–395.
2. Tamm LK, Han X, Li Y, Lai AL. Structure and function of membrane fusion peptides. *Biopolymers* 2002;66:249–260.
3. Lindgren M, Hallbrink M, Prochiantz A, Langel U. Cell penetrating peptides. *Trends Pharm Sci* 2000;21:99–103.
4. Zheng N, Gierasch LM. Signal sequences: the same yet different. *Cell* 1996;86:849–852.
5. Yip CM, Darabie AA, McLaurin J. A $\beta$ 42-peptide assembly on lipid bilayers. *J Mol Biol* 2002;318:97–107.



6. Volles MJ, Lansbury PT Jr. Zeroing in on the pathogenic form of  $\alpha$ -synuclein and its mechanism of neurotoxicity in Parkinson's disease. *Biochemistry* 2003;42:7871–7878.
7. Bernéche S, Nina M, Roux B. MD simulation of melittin in a DMPC bilayer membrane. *Biophys J* 1998;75:1603–1618.
8. Tieleman DP, Borisenko V, Sansom MSP, Woolley GA. Understanding pH-dependent selectivity of alamethicin K18 channels by computer simulation. *Biophys J* 2003;84:1464–1469.
9. Shepherd CM, Vogel HJ, Tieleman DP. Interactions of the designed antimicrobial peptide MB21 and truncated dermaseptin S3 with lipid bilayers: MD simulations. *Biochem J* 2003;370:233–243.
10. Aliste MP, MacCallum JL, Tieleman DP. MD simulations of pentapeptides at interfaces: salt bridge and cation- $\pi$  interactions. *Biochemistry* 2003;42:8976–8987.
11. Ben-Tal N, Ben-Shaul A, Nicholls A, Honig B. Free energy determinants of  $\alpha$ -helix insertion into lipid bilayers. *Biophys J* 1996;70:1803–1812.
12. Kessel A, Cafiso DS, Ben-Tal N. Continuum solvent model calculations of alamethicin-membrane interactions: thermodynamic aspects. *Biophys J* 2000;78:571–583.
13. Bechor D, Ben-Tal N. Implicit solvent model studies of the interactions of the influenza hemagglutinin fusion peptide with lipid bilayers. *Biophys J* 2001;80:643–655.
14. Murray D, Ben-Tal N, Honig B, McLaughlin S. Electrostatic interaction of myristoylated proteins with membranes: simple physics, complicated biology. *Structure* 1997;5:985–989.
15. Murray D, McLaughlin S, Honig B. The role of electrostatic interactions in the membrane association of G protein  $\beta$  heterodimers. *J Biol Chem* 2001;276:45153–45159.
16. Ducarme P, Rahman M, Brasseur R. IMPALA: a simple restraint field to simulate the biological membrane in molecular structure studies. *Proteins* 1998;30:357–371.
17. Brasseur R, Deleers M, Malaisse WJ, Ruysschaert J-M. Conformational analysis of the Ca-A23187 complex at a lipid-water interface. *Proc Natl Acad Sci USA* 1982;79:2895–2897.
18. Brasseur R, Pillot T, Lins L, Vandekerckhove J, Rosseneu M. Peptides in membranes: tipping the balance of membrane stability. *TIBS* 1997;22:167–171.
19. Jahnig F, Edholm O. Modeling of the structure of bacteriorhodopsin. *J Mol Biol* 1992;226:837–850.
20. Ram P, Kim E, Thomson DS, Howard KP, Prestegard JH. Computer modeling of glycolipids at membrane surfaces. *Biophys J* 1992;63:1530–1535.
21. Sanders CR, Schwonek JP. An approximate model and empirical energy function for solute interactions with a water-phosphatidylcholine interface. *Biophys J* 1993;65:1207–1218.
22. Milik M, Skolnick J. Spontaneous insertion of peptide chains into lipid membranes: an off-lattice Monte Carlo dynamics model. *Proteins* 1993;15:10–25.
23. Efremov RG, Nolde DE, Vergoten G, Arseniev AS. A solvent model for simulations of peptides in bilayers: I. Membrane-promoting  $\alpha$ -helix formation. *Biophys J* 1999;76:2448–2459.
24. La Rocca P, Biggin PC, Tieleman DP, Sansom MSP. Simulation studies of the interaction of antimicrobial peptides and lipid bilayers. *Biochim Biophys Acta* 1999;1462:185–200.
25. Lazaridis T. Effective energy function for proteins in lipid membranes. *Proteins* 2003;52:176–192.
26. Lazaridis T, Karplus M. Effective energy function for proteins in solution. *Proteins* 1999;35:133–152.
27. Spassov VZ, Yan L, Szalma S. Introducing an implicit membrane in Generalized Born/Solvent Accessibility continuum solvent models. *J Phys Chem B* 2002;106:8726–8738.
28. Im W, Feig M, Brooks CL III. An implicit membrane GB theory for the study of structure, stability, and interactions of membrane proteins. *Biophys J* 2003;85:2900–2918.
29. Gennis RB. *Biomembranes: molecular structure and function*. New York: Springer-Verlag; 1989.
30. Ben-Tal N, Honig B, Miller C, McLaughlin S. Electrostatic binding of proteins to membranes: theoretical predictions and experimental results with charybdotoxin and phospholipid vesicles. *Biophys J* 1997;73:1717–1727.
31. Murray D, Arbutova A, Hangyas-Mihalyne G, Gambhir A, Ben-Tal N, Honig B, McLaughlin S. Electrostatic properties of membranes containing acidic lipids and adsorbed basic peptides: theory and experiment. *Biophys J* 1999;77:3176–3188.
32. Diraviyam K, Stahelin RV, Cho W, Murray D. Computer modeling of the membrane interaction of FYVE domains. *J Mol Biol* 2003;328:721–736.
33. McLaughlin S. The electrostatic properties of membranes. *Ann Rev Biophys Chem* 1989;18:113–136.
34. Israelachvili JN. *Intermolecular and surface forces*. London: Academic Press; 1985.
35. Lazaridis T, Karplus M. “New view” of protein folding reconciled with the old through multiple unfolding simulations. *Science* 1997;278:1928–1931.
36. Neria E, Fischer S, Karplus M. Simulation of activation free energies in molecular systems. *J Chem Phys* 1996;105:1902–1921.
37. Nagle JF, Tristram-Nagle S. Structure of lipid bilayers. *Biochim Biophys Acta* 2000;1469:159–195.
38. Ben-Tal N, Honig B, Bagdassarian CK, Ben-Shaul A. Association entropy in adsorption processes. *Biophys J* 2000;79:1180–1187.
39. White SH, Wimley WC. Membrane protein folding and stability: physical principles. *Ann Rev Biophys Biomol Struct* 1999;28:319–365.
40. Ben-Tal N, Honig B, Peitzsch RM, Denisov G, McLaughlin S. Binding of small basic peptides to membranes containing acidic lipids. *Biophys J* 1996;71:561–575.
41. Victor KG, Cafiso DS. Location and dynamics of basic peptides at the membrane interface: EPR of TOAC-labeled peptides. *Biophys J* 2001;81:2241–2250.
42. May S, Harries D, Ben-Shaul A. Lipid demixing and protein-protein interactions in the adsorption of charged proteins on mixed membranes. *Biophys J* 2000;79:1747–1760.
43. Batenburg AM, van Esch JH, de Kruijff B. Melittin-induced changes of the macroscopic structure of PE. *Biochemistry* 1988;27:2324–2331.
44. Kuchinka E, Seelig J. Interaction of melittin with PC membranes: binding isotherm and lipid head-group conformation. *Biochemistry* 1989;28:4216–4221.
45. Beschiaschvili G, Seelig J. Melittin binding to mixed PC/PG membranes. *Biochemistry* 1990;29:52–58.
46. Wenk MR, Seelig J. Magainin 2 amide interaction with lipid membranes: calorimetric detection of peptide binding and pore formation. *Biochemistry* 1998;37:3909–3916.
47. Wierprecht T, Beyer mann M, Seelig J. Binding of antibacterial magainin peptides to electrically neutral membranes: thermodynamics and structure. *Biochemistry* 1999;38:10377–10387.
48. Magzoub M, Eriksson LEG, Graslund A. Conformational states of penetratin when interacting with phospholipid vesicles. *Biochim Biophys Acta* 2002;1563:53–63.
49. Persson D, Thoren PEG, Herner M, Lincoln P, Norden B. Application of a novel analysis to measure the binding of the membrane-translocating peptide penetratin to negatively charged liposomes. *Biochemistry* 2003;42:421–429.
50. Brattwall CEB, Lincoln P, Norden B. Orientation and conformation of cell-penetrating peptide penetratin in phospholipid vesicle membranes determined by polarized light spectroscopy. *J Am Chem Soc* 2003;125:14214–14215.
51. Raussens V, Slupsky CM, Sykes BD, Ryan RO. Lipid-bound structure of an apolipoprotein E-derived peptide. *J Biol Chem* 2003;278:25998–26006.
52. Chien K-Y, Chiang C-M, Hseu Y-C, Vyas AA, Rule GS, Wu W-G. Two distinct types of cardiotoxin as revealed by the structure and activity relationship of their interaction with zwitterionic phospholipid dispersions. *J Biol Chem* 1994;269:14473–14483.
53. Sue S-C, Rajan PK, Chen T-S, Hsieh C-H, Wu W-G. Action of Taiwan cobra cardiotoxin on membranes: binding modes of a  $\beta$ -sheet polypeptide with PC bilayers. *Biochemistry* 1997;36:9826–9836.
54. Sue S-C, Chien K-Y, Huang W-N, Abraham JK, Chen K-M, Wu W-G. Heparin binding stabilizes the membrane-bound form of cobra cardiotoxin. *J Biol Chem* 2002;277:2666–2673.
55. Dubovskii PV, Lesovoy DM, Dubinnyi MA, Utkin YN, Arseniev AS. Interaction of the P-type cardiotoxin with phospholipid membranes. *Eur J Biochem* 2003;270:2038–2046.
56. Huang W-N, Sue S-C, Wang D-S, Wu P-L, Wu W-G. Peripheral binding mode and penetration depth of cobra cardiotoxin on phospholipid membranes as studied by a combined FTIR and computer simulation approach. *Biochemistry* 2003;42:7457–7466.
57. Efremov RG, Volynsky PE, Nolde DE, Dubovskii PV, Arseniev AS. Interactions of cardiotoxins with membranes: a molecular modeling study. *Biophys J* 2002;83:144–153.
58. Dubovskii PV, Dementieva DV, Bocharov EV, Utkin YN, Arseniev

- AS. Membrane binding motif of the P-type cardiotoxin. *J Mol Biol* 2001;305:137–149.
59. Kabsch W, Sander C. Dictionary of protein secondary structure. *Biopolymers* 1983;22:2577–2637.
60. Surewicz WK, Stepanik TM, Szabo AG, Mantsch HH. Lipid-induced changes in secondary structure of snake venom cardiotoxins. *J Biol Chem* 1988;263:786–790.
61. Verwey E JW, Overbeek JTG. Theory of the stability of lyophobic colloids. New York: Elsevier; 1948.
62. Bishop CM, Walkenhorst WF, Wimley WC. Folding of  $\beta$ -sheets in membranes: specificity and promiscuity in peptide model systems. *J Mol Biol* 2001;309:975–988.

## APPENDIX: STANDARD FREE ENERGIES OF MEMBRANE BINDING

Most experimental studies of peptide partitioning between aqueous solution and membranes report either the mole fraction partition coefficient

$$K_x = X_b / X_w$$

where  $X_b$  and  $X_w$  are the mole fractions of the peptide in the membrane and in water, respectively; or the apparent partition coefficient

$$K_{app} = X_b / C_w$$

where  $C_w$  is the molarity of the free peptide in bulk solution. The relationship between the two is

$$K_x \approx K_{app}(55.5M)$$

The standard free energies corresponding to these partition coefficients are

$$\Delta G_{app}^o = -RT \ln K_{app}$$

$$\Delta G_x^o = -RT \ln K_x,$$

and the relationship between the two,

$$\begin{aligned} \Delta G_{app}^o &= \Delta G_x^o + RT \ln(55.5) \\ &= \Delta G_x^o + 2.41 \text{ kcal/mol (at } T = 300K). \end{aligned}$$

The term  $RT \ln(55.5)$  is sometimes called the “cratic entropy.”

A third type, the molar partition coefficient, is defined as

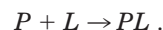
$$K_c = C_b / C_w$$

where  $C_b$  is the molarity in the lipid phase. The standard free energy at 1 *M* standard state is

$$\Delta G_c^o = -RT \ln(K_c) = \Delta G_x^o + RT \ln(V_L/V_w),$$

where  $V_L$  and  $V_w$  are the molar volumes of a lipid molecule and water, respectively. Using  $V_L \approx 1000 \text{ \AA}^3$  and  $V_w = 30 \text{ \AA}^3$ , we obtain  $\Delta G_c^o = \Delta G_x^o + 2.1 \text{ kcal/mol}$ .<sup>39</sup> From the above equations, it can be seen that  $\Delta G_c^o$  is numerically very close to  $\Delta G_{app}^o$ .

Peptide binding to membranes can also be treated as peptide–lipid binding:



The equilibrium constant for this process is equivalent to the apparent partition coefficient defined above:

$$K = \frac{[PL]}{[P][L]} = \frac{[P]_{bound}}{[P]_{free}[L]} = \frac{X_{bound}}{[P]_{free}} \approx K_{app}.$$

The standard free energy of binding can be written

$$\Delta G^o = \Delta \langle W \rangle - T \Delta S^{\text{tr-rot-conf}}$$

where  $\Delta \langle W \rangle$  is the change in effective energy (containing the interactions of the peptide with its surroundings) and  $\Delta S^{\text{tr-rot-conf}}$  is the change in translational, rotational, and conformational entropy upon binding. The translational entropy term depends on the standard state chosen. Ben-Tal et al.<sup>38</sup> calculated the translational and rotational entropy terms for peptide adsorption onto a membrane for the 1 *M* standard state and found them to be about  $-1.3 \text{ kcal/mol}$ . Therefore, if conformational entropy changes can be neglected, we expect  $\Delta G_c^o$  or  $\Delta G_{app}^o$  to be about  $1.3 \text{ kcal/mol}$  more positive than the  $\Delta \langle W \rangle$  term calculated in this work.

Reports of binding of charged peptides to membranes often attempt to separate the binding process into two steps: accumulation next to the membrane due to the electrostatic potential (computed using the GC theory), and insertion into the membrane. The second step is characterized by an intrinsic binding constant,  $K_p$ . In this work, we do not adopt this separation; therefore, we compare to the overall partitioning coefficients,  $K_{app}$ . The standard free energies used in this article for comparison with the theoretical results correspond to  $\Delta G_{app}^o = -RT \ln K_{app}$ .